



Input from the SND@LHC collaboration to the 2026 Update to the European Strategy for Particle Physics

SND@LHC Collaboration

April 1, 2025

By observing collider neutrino interactions of different flavours, the SND@LHC and Faser ν experiments have shown that the LHC can make interesting contributions to neutrino physics. This document summarizes why the SND@LHC Collaboration intends to continue taking data at the High Luminosity LHC (HL-LHC).

The upgraded detector[1] will instrument the regions of both the neutrino vertex and the magnetized calorimeter with silicon microstrips. The use of this technology will allow us to continue the physics program of the current SND@LHC detector with higher statistics. It will also offer new possibilities. For instance, the magnetization of the hadron calorimeter will enable the separation between neutrinos and antineutrinos. This could lead to the first direct observation of tau antineutrinos.

The use of ultrafast timing layers will enable triggers to be sent to ATLAS, potentially allowing the identification of the charm quark pair that produced the neutrino interacting in the detector. Such tagging of the neutrino source would fulfill Pontecorvo's original proposal of a tagged neutrino beam. The experiment will perform unique measurements with high energy neutrinos and will also provide a means to measure gluon parton distribution functions in a previously unexplored domain (Bjorken- $x < 10^{-5}$).

Furthermore, the technological advancements of the upgrade and the experience that will be gained in the areas of operation and data analysis will play a crucial role in the design of the neutrino detector for the SHiP experiment.

D. Abbaneo⁹, C. Ahdida⁹, S. Ahmad⁴², R. Albanese^{1,2}, A. Alexandrov¹,
 F. Alicante^{1,2}, F. Aloschi^{1,2}, N. Amapane^{14,15}, M. Andreini⁹, K. Androsov⁶,
 A. Anokhina³, T. Asada³⁴, C. Asawatangtrakuldee³⁸, M.A. Ayala Torres^{27,32},
 N. Bangaru^{1,2,9}, C. Battilana^{4,5}, A. Bay⁶, A. Bertocco^{1,2}, C. Bertone⁹, C. Betancourt⁷,
 D. Bick⁸, R. Biswas⁹, A. Blanco Castro¹⁰, V. Boccia^{1,2}, O. Boettcher⁹,
 M. Bogomilov¹¹, D. Bonacorsi^{4,5}, W.M. Bonivento¹², P. Bordalo¹⁰, A. Boyarsky^{13,14},
 T.A. Bud⁹, L. Buonocore⁹, S. Buontempo¹, V. Cafaro⁴, T. Camporesi^{10,52}, V. Canale^{1,2},
 D. Centanni^{1,16}, F. Cerutti⁹, A. Cervelli⁴, V. Chariton⁹, N. Charitonidis⁹,
 M. Chernyavskiy³, A. Chiuchiolo¹, K.-Y. Choi¹⁷, S. Cholak⁶, F. Cindolo⁴,
 M. Climescu¹⁸, A.P. Conaboy¹⁹, O. Crespo Lopez⁹, A. Crupano⁴, D. D'Agostino¹,
 G.M. Dallavalle⁴, N. D'Ambrosio⁴⁵, D. Davino^{1,20}, R. De Asmundis¹, P.T. de Bryas⁶,
 G. De Lellis^{1,2}, M. De Magistris^{1,16}, G. De Marzi¹, S. De Pasquale^{1,46}, A. De Roeck⁹,
 A. De Rújula⁹, D. De Simone⁷, A. Di Crescenzo^{1,2}, D. Di Ferdinando⁴, L. Di Giulio⁹,
 S. di Luca⁹, C. Dinc²³, R. Donà^{4,5}, O. Durhan^{23,43}, D. Fasanella⁴, M. Ferrillo⁷,
 R.A. Fini²¹, A. Fiorillo^{1,2}, R. Fresa^{1,24}, W. Funk⁹, N. Funicello¹, C. Gaignant⁹,
 V. Giordano⁴, A. Golutvin²⁶, E. Graverini^{6,41}, L. Guiducci^{4,5}, A.M. Guler²³,
 V. Guliaeva³⁷, G.J. Haefeli⁶, C. Hagner⁸, J.C. Helo Herrera^{27,40}, A. Herty⁹,
 E. van Herwijnen²⁶, A. Iaiunese^{1,2}, S. Ilieva^{9,11}, A. Infantino⁹, A. Iuliano^{1,2},
 H. Jeangros⁹, C. Kamiscioglu²³, A.M. Kauniskangas⁶, S.H. Kim²⁹, Y.G. Kim³⁰,
 G. Klioutchnikov⁹, M. Komatsu³¹, S. Kuleshov^{27,32}, L. Krzempek^{1,2,9}, H.M. Lacker¹⁹,
 O. Lantwin¹, F. Lasagni Manghi⁴, A. Lauria^{1,2}, K.Y. Lee²⁹, K.S. Lee³³, P. Lelong⁹,
 E. Leo¹, G. Lerner⁹, V.P. Loschiavo^{1,20}, G. Magazzù⁴⁷, M. Majstorovic⁹, S. Marcellini⁴,
 A. Margiotta^{4,5}, A. P. Marion⁹, A. Mascellani⁶, F. Mei⁵, A. Miano^{1,44},
 A. Mikulenko¹³, M.C. Montesi^{1,2}, F.L. Navarria^{4,5}, E. Nowak⁹, W. Nuntiyakul³⁹,
 S. Ogawa³⁴, J. Osborne⁹, M. Ovchinnikov⁹, G. Paggi^{4,5}, K. Pal⁹, J. Panigoni⁹,
 B.D. Park²⁹, S. Pelletier⁹, M. Perez Ornedo⁹, A. Perrotta⁴, N. Polukhina³,
 F. Primavera⁴, A. Prota^{1,2}, O. Prouteau⁹, A. Quercia^{1,2}, S. Ramos¹⁰, A. Reghunath¹⁹,
 F. Ronchetti⁶, L. Rottoli^{50,51}, T. Rovelli^{4,5}, O. Ruchayskiy³⁵, M. Sabate Gilarte⁹,
 Z. Sadykov¹, F. Sanchez Galan⁹, M. Sarno^{1,46}, V. Scalerà^{1,16}, W. Schmidt-Parzefall⁸,
 O. Schneider⁶, G. Sekhniaidze¹, N. Serra⁷, M. Shaposhnikov⁶, T. Shchedrina^{1,2},
 L. Shchutska⁶, H. Shibuya^{34,36}, A. Sidoti^{4,5}, G. P. Siroti^{4,5}, G. Sirri⁴, G. Soares¹⁰,
 J.Y. Sohn²⁹, O.J. Soto Sandoval^{27,40}, J.L. Soto Pezoa^{27,32}, M. Spurio^{4,5},
 J. Steggemann⁶, M. Szewczyk⁹, I. Timiryasov³⁵, V. Tioukov¹, M. Tobar^{27,32},
 F. Tramontano^{1,2}, C. Trippel⁶, A. Uluwita⁹, E. Ursov¹⁹, G. Vankova-Kirilova¹¹,
 G. Vasquez⁷, V. Verguilov¹¹, N. Viegas Guerreiro Leonardo¹⁰, C. Vilela¹⁰, A. Vieille⁹,
 C. Visone^{1,2}, R. Wanke¹⁸, E. Yaman²³, Z. Yang⁶, E. Yaman^{1,2}, C. Yazici^{1,2},
 C.S. Yoon²⁹, E. Zaffaroni⁶, J. Zamora Saa^{27,32}, M. Zanetti^{48,49}

¹Sezione INFN di Napoli, Napoli, 80126, Italy

²Università di Napoli "Federico II", Napoli, 80126, Italy

³Affiliated with an institute formerly covered by a cooperation agreement with CERN

⁴Sezione INFN di Bologna, Bologna, 40127, Italy

⁵Università di Bologna, Bologna, 40127, Italy

⁶Institute of Physics, EPFL, Lausanne, 1015, Switzerland

- ⁷*Physik-Institut, UZH, Zürich, 8057, Switzerland*
- ⁸*Hamburg University, Hamburg, 22761, Germany*
- ⁹*European Organization for Nuclear Research (CERN), Geneva, 1211, Switzerland*
- ¹⁰*Laboratory of Instrumentation and Experimental Particle Physics (LIP), Lisbon, 1649-003, Portugal*
- ¹¹*Faculty of Physics, Sofia University, Sofia, 1164, Bulgaria*
- ¹²*Università degli Studi di Cagliari, Cagliari, 09124, Italy*
- ¹³*University of Leiden, Leiden, 2300RA, The Netherlands*
- ¹⁴*INFN, Sezione di Torino, Torino, Italy*
- ¹⁵*Università di Torino, Torino, Italy*
- ¹⁶*Università di Napoli Parthenope, Napoli, 80143, Italy*
- ¹⁷*Sungkyunkwan University, Suwon-si, 16419, Korea*
- ¹⁸*Institut für Physik and PRISMA Cluster of Excellence, Mainz, 55099, Germany*
- ¹⁹*Humboldt-Universität zu Berlin, Berlin, 12489, Germany*
- ²⁰*Università del Sannio, Benevento, 82100, Italy*
- ²³*Middle East Technical University (METU), Ankara, 06800, Turkey*
- ²⁴*Università della Basilicata, Potenza, 85100, Italy*
- ²⁶*Imperial College London, London, SW72AZ, United Kingdom*
- ²⁷*Millennium Institute for Subatomic physics at high energy frontier-SAPHIR, Santiago, 7591538, Chile*
- ²⁹*Department of Physics Education and RINS, Gyeongsang National University, Jinju, 52828, Korea*
- ³⁰*Gwangju National University of Education, Gwangju, 61204, Korea*
- ³¹*Nagoya University, Nagoya, 464-8602, Japan*
- ³²*Center for Theoretical and Experimental Particle Physics, Facultad de Ciencias Exactas, Universidad Andrés Bello, Fernandez Concha 700, Santiago, Chile*
- ³³*Korea University, Seoul, 02841, Korea*
- ³⁴*Toho University, Chiba, 274-8510, Japan*
- ³⁵*Niels Bohr Institute, Copenhagen, 2100, Denmark*
- ³⁶*Present address: Faculty of Engineering, Kanagawa, 221-0802, Japan*
- ³⁷*Constructor University, Bremen, 28759, Germany*
- ³⁸*Chulalongkorn University, Bangkok, 10330, Thailand*
- ³⁹*Chiang Mai University, Chiang Mai, 50200, Thailand*
- ⁴⁰*Departamento de Física, Facultad de Ciencias, Universidad de La Serena, La Serena, 1200, Chile*
- ⁴¹*Also at: Università di Pisa, Pisa, 56126, Italy*
- ⁴²*Present address: Pakistan Institute of Nuclear Science and Technology (PINSTECH), Nilore, 45650, Islamabad, Pakistan*
- ⁴³*Also at: Atılım University, Ankara, Turkey*
- ⁴⁴*Present address: Pegaso University, Napoli, Italy*
- ⁴⁵*Laboratori Nazionali dell'INFN di Gran Sasso, L'Aquila, Italy*
- ⁴⁶*Università di Salerno, Salerno, 84084, Italy*
- ⁴⁷*INFN, Sezione di Pisa, I-56127 Pisa, Italy*
- ⁴⁸*INFN, Sezione di Padova, Padova, Italy*
- ⁴⁹*Università di Padova, Padova, Italy*
- ⁵⁰*Università degli Studi di Milano-Bicocca, Milano Italy*
- ⁵¹*INFN, Sezione di Milano-Bicocca, Milano, Italy*
- ⁵²*Physics Department, Boston University, USA*

1 Introduction

The upgraded SND@LHC detector for the HL-LHC phase (hereafter named SND@HL-LHC for brevity) is designed to identify all three neutrino flavors and to measure their energy. It consists of a target and a magnetized calorimeter (Figure 1). The Tungsten-Silicon sandwich of the target serves as both an electromagnetic calorimeter and a vertex detector, distinguishing neutrino interaction and tau decay vertices. The Iron-Silicon sandwich of the magnetized calorimeter measures hadronic energy, identifies muons from ν_μ interactions and tau decays, and determines their energy.

Compared to the current SND@LHC detector, the proposed setup features three major upgrades:

1. The use of silicon strip modules recovered from the decommissioned CMS Outer Barrel tracker to equip both the vertex detector and the magnetic spectrometer as active element.
2. The addition of four fast timing detector layers in the target to trigger the readout of the silicon detectors and to send a trigger to ATLAS for the tagging of the neutrino parent.
3. The magnetized hadron calorimeter will allow for precise ($\approx 20\%$ at 1 TeV) muon momentum measurements.

The existing veto system will be used to reject charged particles and tag muon for calibration purposes.

The target consists of 58 tungsten plates (7 mm thick) alternating with 58 silicon tracker layers, covering $40 \times 40 \text{ cm}^2$, totaling 1.3 tons and 116 radiation lengths (X_0). The segmented electromagnetic calorimeter ensures efficient ν_e CC interaction identification.

The magnetized hadron calorimeter has 34 iron walls (5 cm thick) interleaved with silicon tracker layers, totaling 8 interaction lengths (λ_{int}). A 1.8 T vertical magnetic field enables muon charge and momentum measurement, distinguishing neutrinos from anti-neutrinos and enhancing physics capabilities.

The proposed detector is designed to fit entirely within the existing TI18 tunnel.

It is worth noting that a modest civil engineering work, with an excavation of 4.5 cubic meters, would improve by a factor ≈ 7 the accumulated statistics and hence the physics reach, in particular in the ν_τ sector.

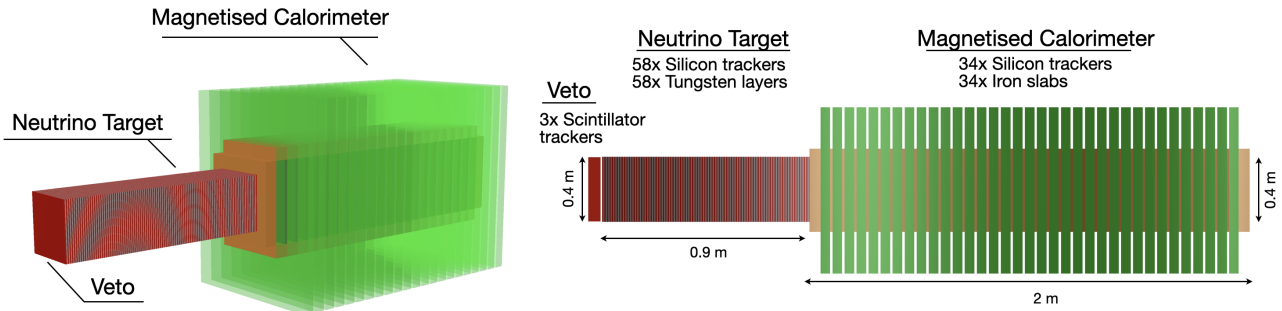


Figure 1: Layout of the upgraded SND@LHC detector, as implemented in the 3D simulation.

2 Physics goals

SND@HL-LHC aims to exploit the large neutrino flux in the forward region of pp collisions at HL-LHC to study neutrino production and interaction mechanisms. Its large cross-sectional area covers a broad pseudo-rapidity range, enabling measurements at lower pseudo-rapidities where charm hadron decays dominate. The experiment, over the full HL-LHC period, will detect thousands of ν_μ and ν_e interactions and a few hundred ν_τ interactions, with energies up to a few TeV. Neutrino spectra are shown in Figure 2, with CC DIS interaction spectra in the right panel.

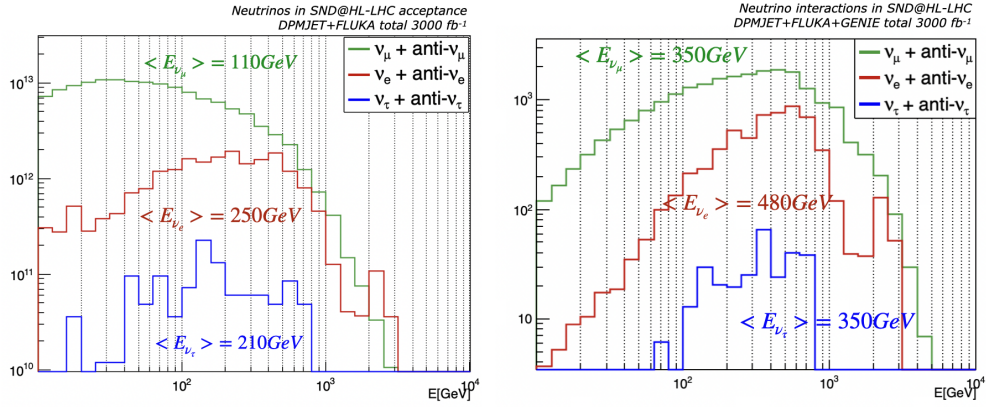


Figure 2: Energy spectra of the three neutrino flavours in the target acceptance (left) and undergoing CC DIS interactions in the target (right). The normalization corresponds to 3000 fb^{-1} . Average energies are also reported.

SND@HL-LHC expects a high event rate of all three neutrino flavors, enabling Lepton Flavour Universality (LFU) tests via interaction ratios. The ν_τ to ν_e ratio, dominated by charmed hadron decays, will be statistically limited, while the ν_e to ν_μ ratio will have high precision but systematic uncertainties from pion-decay contamination. **These complementary measurements will allow precise LFU tests with all three neutrino flavors.**

High-energy ν_e from charm decays enable studies of forward charm production in pp collisions, **probing the gluon Parton Density Function (PDF) at Bjorken x below 10^{-5} .** Constraining the gluon PDF in this regime improves cosmic neutrino background models and predictions for future high-energy hadron colliders. Aside from future hadron colliders and HL-LHC neutrino experiments, no other current or planned experiments access such small x values.

High-statistics cross-section measurements will be conducted for the highest-energy neutrinos ever produced by human-made sources. Tau neutrino interactions are particularly significant, with potential for unprecedented event collection. Notably, SND@HL-LHC may **achieve the first direct observation of the tau antineutrino.** The large ν_τ flux will also **enable competitive limits on its magnetic moment** via neutrino elastic scattering on electrons [2].

Correlations between neutrinos detected in SND@HL-LHC and ATLAS data will be explored. In particular, a few hundred open charm production events are expected to emit a charm hadron in the ATLAS detector acceptance in coincidence with a neutrino interaction in SND@HL-LHC. **This charm-tagging approach allows for the selection of a sample of**

neutrinos with charm-hadron origin. Such a sample can be used in LFU tests with clean ratios greatly reducing the systematic uncertainty.

Finally, SND@HL-LHC is also sensitive to new physics scenarios, particularly in **scattering signatures of feebly interacting particles**. This approach relies on searching for excesses in the rates of processes that are well predicted by the Standard Model, such as the ratio of neutral current to charged current neutrino interactions, and neutrino scattering on electrons [3].

3 Physics performances

3.1 Neutrino yields

The neutrino yields at the target region for the three different neutrino flavours are reported in the left column of Table 1. An integrated luminosity of 3000 fb^{-1} and the $+250 \text{ } \mu\text{rad-H}$ beam configuration are assumed.

The expected number of CC and NC neutrino interactions occurring in the detector target assuming a 1.3 ton tungsten mass is reported in Table 1.

The neutrino component produced in charmed hadron decays was also estimated using the PYTHIA8 [4] and POWHEG [5] generators activating hard QCD processes only, which provide a number of expected neutrino interactions $20 \div 30\%$ less with respect to DPMJET in the pseudorapidity range of SND@HL-LHC. Beyond the differences in the expected number of interactions, subtle variations can be observed in the ratio of neutrino to antineutrino fluxes, likely arising from different hadronization models. The ability of SND@HL-LHC to distinguish between ν and $\bar{\nu}$ will aid in refining these models.

Flavour	CC DIS			NC DIS		
	DPMJET		POWHEG+P8	DPMJET		POWHEG+P8
	π/K	charm		π/K	charm	
ν_μ	9.6×10^3	1.4×10^3	1.5×10^3	3.0×10^3	4.2×10^2	4.4×10^2
$\bar{\nu}_\mu$	3.1×10^3	9.9×10^2	6.8×10^2	1.1×10^3	3.7×10^2	2.5×10^2
ν_e	5.0×10^2	1.6×10^3	1.5×10^3	1.4×10^2	4.9×10^2	4.5×10^2
$\bar{\nu}_e$	2.0×10^2	1.1×10^3	6.9×10^2	6.0×10^1	4.2×10^2	2.5×10^2
ν_τ	—	2.2×10^2	9.3×10^1	—	7.6×10^1	3.0×10^1
$\bar{\nu}_\tau$	—	5.7×10^1	5.0×10^1	—	2.5×10^1	2.0×10^1
Tot	1.3×10^4	5.4×10^3	4.5×10^3	4.3×10^3	1.8×10^3	1.4×10^3

Table 1: Number of CC DIS and NC DIS neutrino interactions, assuming 3000 fb^{-1} , as estimated with DPMJET/FLUKA, POWHEG+P8 and GENIE generators.

It has to be noted that a large number of neutrino interactions will occur also in the HCAL. The high granularity of the silicon trackers will make the upstream part of the HCAL a good target to identify muon- and ν_e s interactions thus adding to the overall neutrino interactions statistics.

Preliminary estimates based on the longitudinal development of hadronic and electromagnetic showers in the HCAL show that about 40% of muon and ν_e s interacting in Iron layers are fully contained in the detector — with the exception of the muon produced in ν_μ CC DIS

interactions. The right panel of Figure 3 shows the fraction of ν_e CC DIS interactions occurring in the HCAL that have a longitudinal development fully contained in the detector, as a function of the interaction position. A display of one of those is shown in the left panel of the same figure. The corresponding neutrino yield is reported in Table 2, assuming 3000 fb^{-1} and the $+250 \text{ } \mu\text{rad-H}$ beam configuration. This indicates a potential increase of about 50% of detectable neutrino interactions.

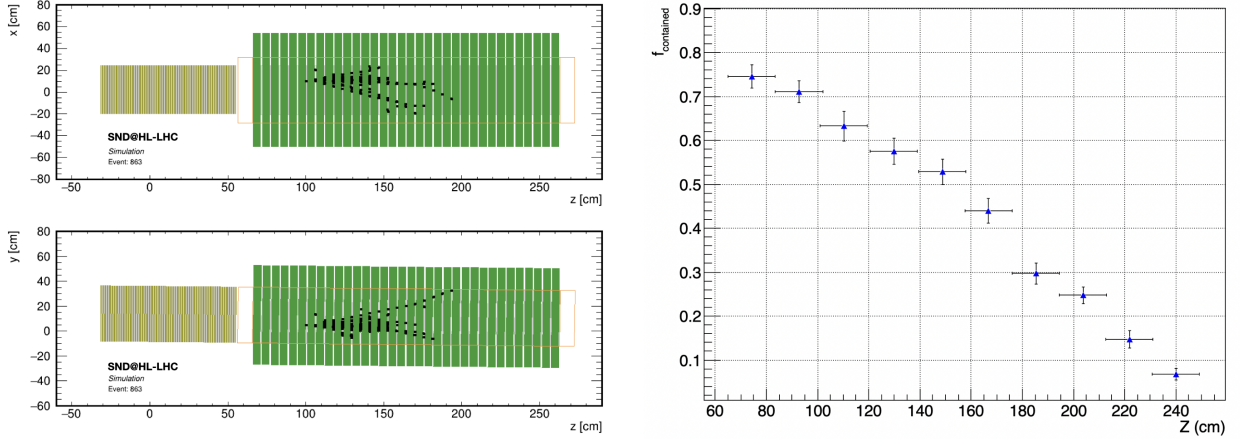


Figure 3: Left: display of an ν_e interaction occurring in the HCAL. Right: fraction of ν_e CC DIS interactions occurring in the HCAL and fully contained in the detector, as a function of the longitudinal position of the interaction.

Flavour	Target	HCAL	Target+HCAL
$\nu_\mu + \bar{\nu}_\mu$	1.5×10^4	8.8×10^3	2.4×10^4
$\nu_e + \bar{\nu}_e$	3.4×10^3	2.1×10^3	5.5×10^3
$\nu_\tau + \bar{\nu}_\tau$	2.8×10^2	1.7×10^2	4.5×10^2
Tot	1.9×10^4	1.1×10^4	3.0×10^4

Table 2: Number of neutrinos CC DIS interactions in the Target and in the HCAL, assuming 3000 fb^{-1} and the $+250 \text{ } \mu\text{rad-H}$ configuration. Longitudinal shower containment is required for interactions in the HCAL.

3.2 Neutrino physics

Electron neutrinos in the SND@HL-LHC pseudo-rapidity range $6.9 < \eta < 7.7$ are mostly produced by charm decays. Therefore, ν_e s can be used as a probe of charm production in an angular range where the charm yield has a large uncertainty, to a large extent coming from the gluon parton distribution function (PDF). Electron neutrino measurements can thus constrain the uncertainty on the gluon PDF in the very small (below 10^{-5}) Bjorken x region (see Figure 4). The interest therein is two-fold: firstly, the gluon PDF in this x domain will be relevant for Future Circular Collider (FCC) experiments; secondly, the measurement will

reduce the uncertainty on the flux of very high energy (\sim PeV) atmospheric neutrinos produced in charm decays, essential for the evidence of neutrinos from astrophysical sources [6], [7]. The charm measurement by the current detector in Run 3 will be affected by a systematic

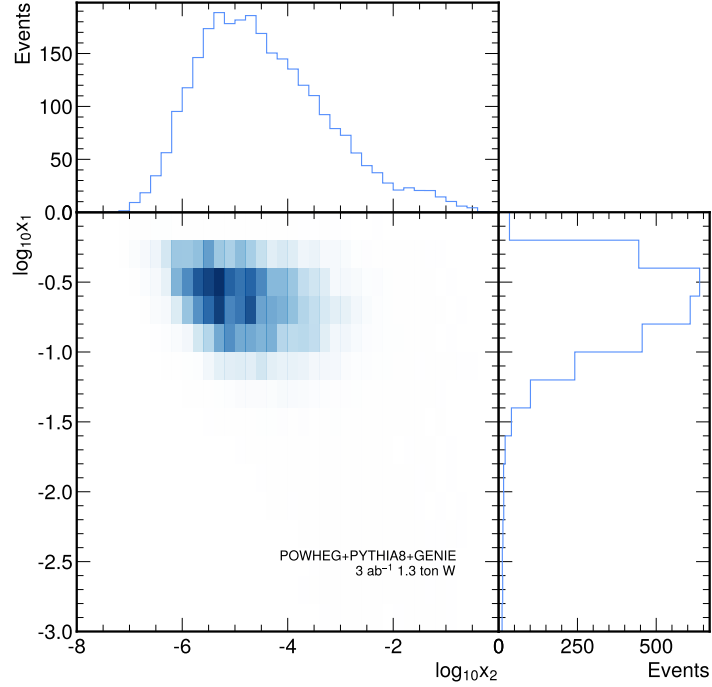


Figure 4: Distribution of Bjorken x of the colliding partons in open charm production events resulting in an ν_e charged current interaction in SND@HL-LHC. The events were generated with POWHEG, with parton shower modeling by PYTHIA8 and the ν_e charged current cross section from GENIE.

uncertainty of 35% and by a statistical uncertainty of almost 10%. The operation in HL-LHC of the SND@LHC detector will reduce the statistical uncertainty to about 2%, as is clear from Table 1. The combination of a large number of ν_e events with charm origin, and the wide range of pseudo-rapidity covered by SND@HL-LHC allows for constraining PDFs using correlations of neutrino event rates between energy and pseudo-rapidity bins. Theory uncertainties that have a large impact on the overall event rate normalization, such as the renormalization and factorization scales and the charm quark mass, largely cancel out in shape-based measurements of the PDF, as demonstrated in Figure 5.

We estimate the systematic uncertainty of approximately 5% in the gluon PDF measurement by considering the scale of non-PDF theory parameter variations within bins of the shape-only distribution.

The SND@HL-LHC detector’s ability to identify all three neutrino flavours enables testing Lepton Flavour Universality in neutrino interactions.

Figure 6 shows ν_μ and ν_e spectra within the detector’s acceptance, with heavy-quark decay contributions as the filled area.

At the Target, ν_e s from pion and kaon decays constitute 34% of the total flux but contribute only 20% of interactions due to lower energies and cross-sections. Assuming tau and ν_e s orig-

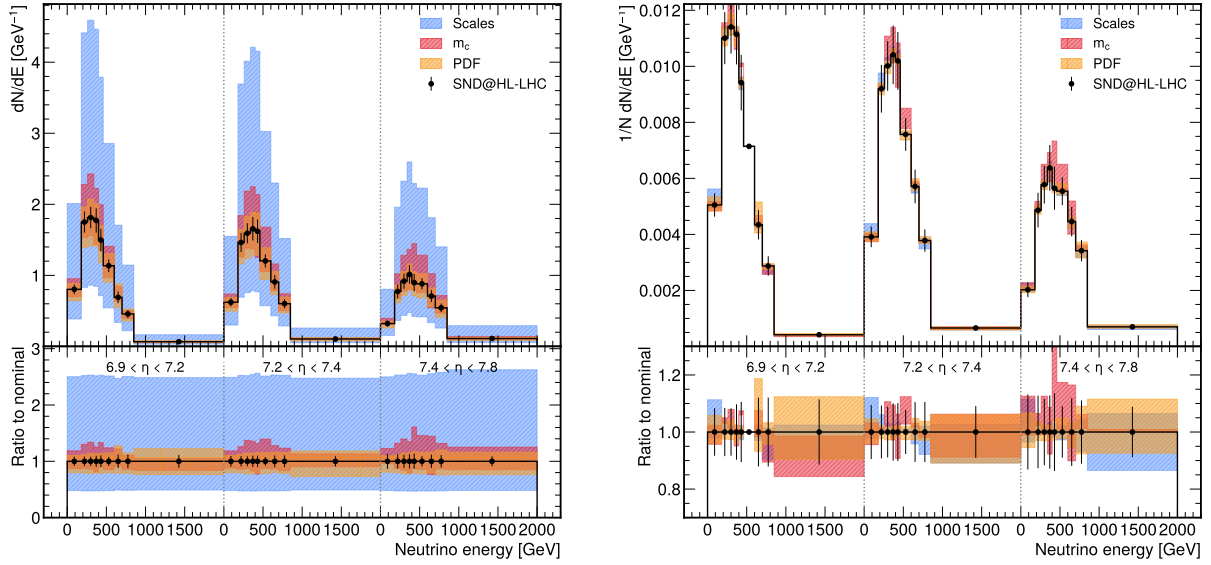


Figure 5: Distribution of energy and pseudo-rapidity of charged-current interactions of ν_e s of charm-hadron origin, simulated at parton level with POWHEG, with parton shower modeling by PYTHIA8 and neutrino interaction cross sections from GENIE. Three sets of systematic uncertainty related to forward charm production are shown: the renormalization and factorization scales (varied to one half and double of the nominal values), the charm quark mass (varied between 1.25 and 1.65 GeV/ c^2), and variations of the PDF based on Ref. [5]. The figure on the left shows the event yield for 3000 fb $^{-1}$, and the figure on the right shows distribution normalized to an arbitrarily chosen reference bin ($460 < E_\nu < 600$ GeV, $6.9 < \eta < 7.2$), emphasizing the impact of systematic variations on the shape of the distribution.

inate from charmed hadron decays, the ν_e to ν_τ ratio (R_{13}) depends on branching ratios and charm fractions, making it sensitive to their cross-section ratio and allowing an Lepton Flavour Universality test [8].

Currently, a 30% statistical uncertainty from low ν_τ statistics dominates. At the HL-LHC SND@HL-LHC will reduce this to 6% (Table 1). The main systematic uncertainty, 20% from D_s fragmentation functions, will improve with ongoing NA65 [9], SHiP-charm [10], and LHCb analyses.

Lepton flavour universality can also be tested using the ν_e -to- ν_μ ratio (R_{12}). With an energy cut, charm can serve as a ν_μ source. Assuming a 600 GeV threshold in the SND@LHC pseudo-rapidity region, a 10% accuracy is expected for both systematic and statistical uncertainties.

The R_{12} measurement at SND@HL-LHC will be optimised to minimize contamination from light hadron decays while reducing statistical uncertainty to a few percent. The strategy involves constraining low-energy ν_μ flux via LHCf [11], achieving better than 10% precision. The ratio will be measured in an energy and pseudo-rapidity region where charm dominates, optimizing the fiducial region to limit pion-decay contamination and reduce systematic uncertainty to a few percent.

The high neutrino beam energy results in most interactions occurring via Deep Inelastic Scattering (DIS). DIS cross-sections have been measured at low energies ($E_\nu < 350$ GeV) by beam dump experiments [12] and at high energies ($E_\nu > 6.3$ TeV) by IceCube for ν_μ s [13].

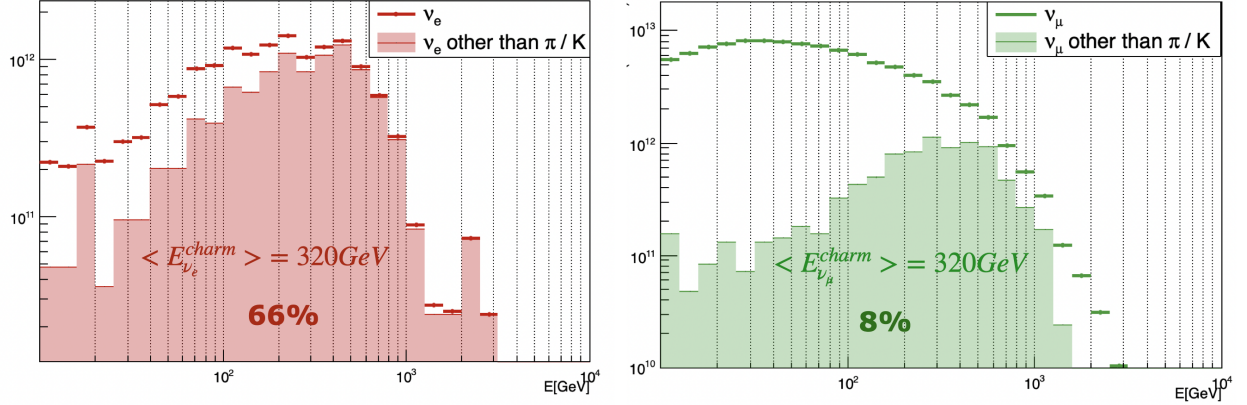


Figure 6: Energy spectrum of ν_μ (right) and ν_e (left) neutrinos and anti-neutrinos in the SND@LH-LHC acceptance. Filled areas represent the component coming from charm decays.

SND@HL-LHC can measure cross-sections in the TeV range using ν_μ s, with precise flux estimates from LHCf light meson production data [14]. The magnetic spectrometer enables charge identification of muons from neutrino CC DIS interactions, allowing separate neutrino and anti-neutrino cross-section measurements up to 1 TeV. At higher energies, the average neutrino energy will be determined.

Figure 7 illustrates SND@HL-LHC's capability to measure the $\nu_\mu N$ cross-section, with statistical uncertainties linked to Table 1 neutrino yields.

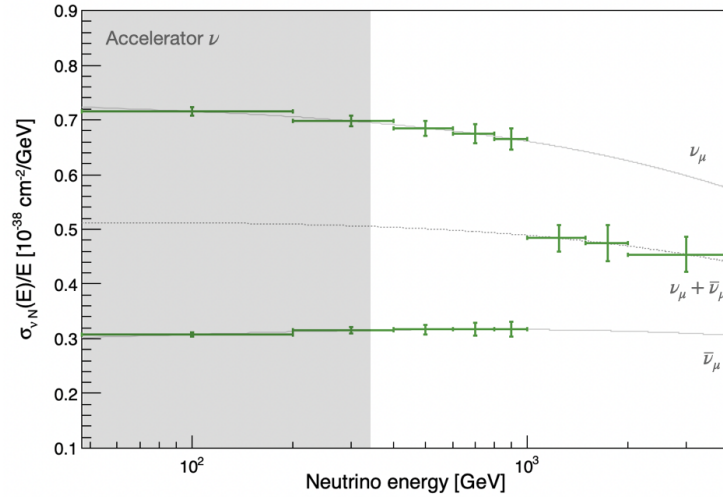


Figure 7: Expected statistical uncertainties for ν_μ CC DIS cross-section measurements. For energies below 1 TeV SND@HL-LHC can distinguish between muon neutrinos and anti-neutrinos. Theoretical predictions are evaluated using GENIE neutrino CC DIS cross-sections on a tungsten Target.

The magnetic moment of neutrinos can be enhanced in some BSM models. The one of the ν_τ is the less constrained due to the lack of data [2].

A larger ν_τ magnetic moment would lead to an increase in the cross section $\sigma_{\nu e}$ for the elastic scattering of neutrinos on electrons, which can be precisely calculated in the SM. An

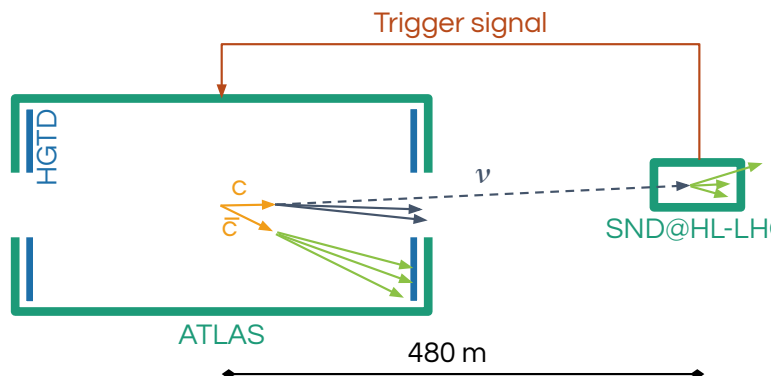


Figure 8: Sketch of a charm-tagged neutrino event in SND@HL-LHC and ATLAS.

enhancement of $\sigma_{\nu e}$ would be a clear signal of new physics. The signature of such events is the presence of a single electron in the final state, with peculiar kinematical features. The SND@HL-LHC detector can efficiently identify electromagnetic showers, and reconstruct their energy and direction. Moreover, the ν_τ flux can be estimated based on the measured yield of ν_τ CC events, and the expected number of single-electron events according to the SM can be constrained by measurements of all flavour neutrinos CC and NC interactions on tungsten. Given the large ν_τ flux produced in p-p collisions at the HL-LHC, the SND@HL-LHC measurements can potentially constrain the ν_τ magnetic moment.

3.3 Charm-tagged neutrino events

The high yield of neutrino events in SND@LHC enables the identification of a sub-sample coinciding with charm hadrons detected in ATLAS. While the neutrino's parent charm hadron is outside ATLAS acceptance, about 10% of associated charm hadrons fall within it, allowing potential detection as sketched in Figure 8. This charm-tagged neutrino sample provides clean flavor ratios with minimal light hadron contamination, enabling LFU tests with lower systematic uncertainty at the expense of higher statistical uncertainty.

PYTHIA8 simulations predict that each bunch crossing with 200 pp collisions at HL-LHC, will produce four charm hadrons within ATLAS acceptance, spread over 200 ps. Neutrino-charm matching requires timing resolution below 50 ps, achievable with ATLAS' Phase-II HGTD upgrade ($2.4 < |\eta| < 4.0$). SND@LHC must therefore have equally or more precise timing detectors.

The left panel of Figure 9 shows the pseudo-rapidity distribution of parton-level charm quark pairs from POWHEG. It highlights events where the most forward charm quark falls within SND@HL-LHC acceptance and the subset where the least central charm quark is within ATLAS HGTD acceptance. Of the forward charm events, 14% also have the other charm quark in HGTD. The right panel includes PYTHIA8 parton showers and GENIE neutrino interactions, showing that 11% of interacting neutrino events contain a charm quark in HGTD acceptance. With 3000 fb^{-1} , 597 neutrino interactions in SND@LHC are expected with an associated charm hadron in ATLAS: 227 ($\nu_e + \bar{\nu}_e$) CC, 212 ($\nu_\mu + \bar{\nu}_\mu$) CC, 10 ($\nu_\tau + \bar{\nu}_\tau$) CC, and 147 NC. These rates enable LFU testing via the charm-tagged $(\nu_e + \bar{\nu}_e)/(\nu_\mu + \bar{\nu}_\mu)$ ratio with 10% statistical precision.

To ensure ATLAS retains data from particles produced alongside neutrinos interacting in SND@LHC, a trigger signal is sent from SND@LHC to ATLAS within the 10 ps latency of the

Measurement	Uncertainty		Uncertainty	
	Stat.	Sys.	Stat.	Sys.
Gluon PDF	5%	35%	2%	5%
ν_e/ν_τ ratio for LFU test	30%	22%	6%	10%
ν_e/ν_μ ratio for LFU test	10%	10%	2%	5%
Charm-tagged ν_e/ν_μ ratio for LFU test	-	-	10%	< 5%
ν_μ and $\bar{\nu}_\mu$ cross-section	-	-	1%	5%

Table 3: SND@HL-LHC neutrino interaction measurements with HL-LHC data vs. Run 3 estimates, including statistical and systematic uncertainties.

upgraded ATLAS trigger. Given the 480 m round-trip time of $3.2 \mu\text{s}$, this signal arrives on time.

Extrapolating from Run 3 data, the expected neutral particle trigger rate at HL-LHC is 1 Hz, negligible for ATLAS. Additionally, reducing light-jet background relies on machine learning-based charm-jet identification, which currently achieves nearly two orders of magnitude light-jet rejection with 40% charm-jet efficiency [15, 16, 17].

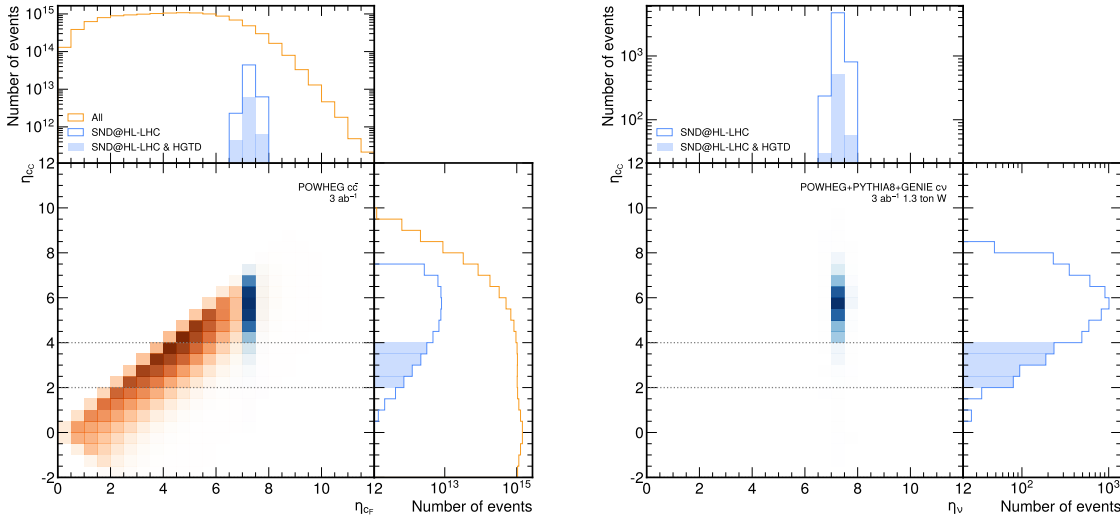


Figure 9: The left figure shows the pseudo-rapidity distribution of the most forward (η_{cF}) and least forward (η_{cC}) charm quarks in pairs from POWHEG. The right figure, including parton shower and neutrino interaction simulations from PYTHIA8 and GENIE, displays the pseudo-rapidity of the most energetic neutrino (η_ν) and η_{cC} . The orange distribution represents the inclusive sample, while blue highlights events within the SND@HL-LHC acceptance. Shaded areas indicate events also detected by ATLAS HGTD. All distributions are normalized to 3 ab^{-1} with a 1.3-ton neutrino target mass.

3.4 Summary of physics results with neutrinos

Table 3 summarises the main HL-LHC physics objectives with the SND@HL-LHC detector in the analyses of neutrino interactions, compared with estimates for the current detector in

Run 3. The proposed measurements are reported together with the estimated uncertainties, as described in detail in the corresponding sections.

4 Conclusion

- SND@HL-LHC will offer a significant contribution to the neutrino physics program at the LHC.
- Upgrading the detector requires a modest investment (< 1 MCHF) by the Collaboration. Parts of the original CMS tracker will be repurposed.
- SND@HL-LHC will test neutrino interactions at the highest accelerator energies, offer unprecedented probes of lepton flavor violation in the neutrino sector, and enhance sensitivity to Beyond Standard Model effects. Additionally, it will improve our understanding of previously unexplored QCD domains and provide valuable insights into charm quark production and the intricacies of its hadronization.

A recognition and endorsement of the SND@HL-LHC programme will be highly beneficial to its successful implementation.

References

- [1] SND@LHC collaboration, *SND@HL-LHC, Scattering and Neutrino Detector in Run 4 of the LHC*, Tech. Rep. [CERN-LHCC-2025-004; LHCC-P-026](#), CERN, Geneva (Mar, 2025).
- [2] DONUT collaboration, *A New upper limit for the tau - neutrino magnetic moment*, *Phys. Lett. B* **513** (2001) 23 [[hep-ex/0102026](#)].
- [3] A. Boyarsky, O. Mikulenko, M. Ovchinnikov and L. Shchutska, *Searches for new physics at SND@LHC*, *JHEP* **03** (2022) 006 [[2104.09688](#)].
- [4] T. Sjöstrand, S. Mrenna and P.Z. Skands, *A Brief Introduction to PYTHIA 8.1*, *Comput. Phys. Commun.* **178** (2008) 852 [[0710.3820](#)].
- [5] L. Buonocore, F. Kling, L. Rottoli and J. Sominka, *Predictions for neutrinos and new physics from forward heavy hadron production at the LHC*, *Eur. Phys. J. C* **84** (2024) 363 [[arXiv 2309.12793](#)].
- [6] W. Bai, M. Diwan, M.V. Garzelli, Y.S. Jeong, K. Kumar and M.H. Reno, *Forward production of prompt neutrinos from charm in the atmosphere and at high energy colliders*, *JHEP* **10** (2023) 142 [[2212.07865](#)].
- [7] R.e.a. Ennerg, *Prompt atmospheric neutrino fluxes: perturbative QCD models and nuclear effects*, *JHEP* **11** (2016) 167.
- [8] C. Ahdida et al., *TECHNICAL PROPOSAL, SND@LHC, Scattering and Neutrino Detector at the LHC*, CERN LHC-2021-003, LHCC-P-016 (24 Feb. 2021) .
- [9] S. Aoki et al., *Dstau: study of tau neutrino production with 400 gev protons from the cern-sps*, *Journal of High Energy Physics* **2020** (2020) .
- [10] SHiP collaboration, *Measurement of associated charm production induced by 400 GeV/c protons*, Scientific Committee Paper [CERN-SPSC-2017-033, SPSC-EOI-017](#), CERN, <http://cds.cern.ch/record/2286844> (2017).
- [11] LHCf COLLABORATION collaboration, *Measurements of longitudinal and transverse momentum distributions for neutral pions in the forward-rapidity region with the lhcf detector*, *Phys. Rev. D* **94** (2016) 032007.
- [12] PARTICLE DATA GROUP collaboration, *Review of Particle Physics*, *PTEP* **2020** (2020) 083C01.
- [13] ICECUBE collaboration, *Measurement of the multi-TeV neutrino cross section with IceCube using Earth absorption*, *Nature* **551** (2017) 596 [[1711.08119](#)].
- [14] LHCf collaboration, *Measurement of forward neutral pion transverse momentum spectra for $\sqrt{s} = 7\text{TeV}$ proton-proton collisions at LHC*, *Phys. Rev. D* **86** (2012) 092001 [[1205.4578](#)].
- [15] S. Mondal and L. Mastrolorenzo, *Machine Learning in High Energy Physics: A review of heavy-flavor jet tagging at the LHC*, [arXiv 2404.01071](#).

- [16] ATLAS collaboration, *ATLAS flavour-tagging algorithms for the LHC Run 2 pp collision dataset*, *Eur. Phys. J. C* **83** (2023) 681 [[arXiv 2211.16345](#)].
- [17] ATLAS collaboration, *Graph Neural Network Jet Flavour Tagging with the ATLAS Detector*, *ATL-PHYS-PUB-2022-027* (2022) .